ELSEVIER

Ecological Modelling 163 (2003) 223–244

ECOLOGICAL MODELLING

www.elsevier.com/locate/ecolmodel

Modelling nitrogen fluxes in oligotrophic environments: NW Mediterranean and NE Atlantic

Nixon Bahamón*, Antonio Cruzado

Oceanography Lab., Centre d'Estudis Avançats de Blanes, Carrer d'accés a la Cala Sant Francesc 14, 17300 Blanes, Spain

Received 01 November 2001; received in revised form 23 October 2002; accepted 06 December 2002

Abstract

Stocks and fluxes of nitrogen in two oligotrophic ecosystems are evaluated using a vertically resolved turbulence-driven ecological model. The model simulates the intra-annual variability of the ecological processes in the upper 300 m of the water column in the Catalan Sea (CS), northwestern Mediterranean, and in the subtropical northeast Atlantic (NEA). Higher irradiance and daylight length making the euphotic layer thicker, together with a higher mixing layer depth explained that the phytoplankton maximum was deeper in NEA than in CS during summertime. In general, the amount of irradiance appears to control the chlorophyll maximum depth while the amount of nitrate transported from the bottom boundary is mainly constraining the phytoplankton stocks. The summer chlorophyll maximum was found at depths below the thermocline and close to the nitracline. In both locations, zooplankton grazing controlled the late winter phytoplankton bloom but reduced more than expected the subsurface phytoplankton concentration in summer. The nitrite maximum was successfully simulated to be close to the chlorophyll maximum, explained by the phytoplankton reduction of nitrate in the dark. The yearly estimates of upward fluxes of nitrate to the euphotic zone were variable depending on the horizon at which fluxes were computed. Just below the euphotic zone, the upward fluxes of nitrate were 0.64 and 0.22 mol N m^{-2} in the CS and NEA, respectively, more closely connected to the variation of the nitrogen gradient than to the density field.

Keywords: Nitrogen; Ecological modelling; Oligotrophic ecosystems; Comparative ecology

1. Introduction

The upper water layers of the open oligotrophic ocean sustain plankton communities contributing to regulate the organic matter fluxes. Such communities are subject to complex interactions of biogeochemical and physical processes taking place in the aquatic environment and the atmosphere still requiring comprehensive interdisciplinary efforts to be well understood (Rastetter, 1996; Carril et al., 1997; Doney, 1999). The phytoplankton community is in charge of producing organic matter from inorganic carbon and nutrients under irradiance conditions higher than 0.5% the irradiance in surface waters, called the euphotic zone. Most of primary production (i.e. 70%) is mainly recycled by means of bacterioplankton decomposition and excretions of zooplankton and higher organisms in the food chain, making up the regenerated production (Dugdale and Goering, 1967). The remaining fraction of non-recycled matter (∼30%) is mainly exported down to deeper waters turning the deep ocean into a large carbon reservoir (Sarmiento et al., 1993). To compensate the exported matter, adjacent ecosystems richer in nitrogen, particularly deeper waters, supply

* Corresponding author. Tel.: +34-972-33-61-01; fax: +34-972-33-78-06.
E-mail address: bahamon@ceab.csic.es (N. Bahamón).

0304-3800/03/$ – see front matter © 2003 Elsevier Science B.V. All rights reserved.
doi:10.1016/S0304-3800(03)00007-3

the system with inorganic nitrogen to generate new production (Lewis et al., 1986).

Nitrate has been widely assumed to be an important predictor of new production in the oligotrophic open ocean (Aufdenkampe et al., 2002) controlling and limiting such a production (Dugdale, 1967; Berges and Falkowski, 1998). In regions of the western Mediterranean Sea with permanent geostrophic fronts, new primary production has been often associated to the turbulent transport of nitrate from deeper waters (Lohrenz et al., 1988; Zakardjian and Prieur, 1994, 1998; Salat, 1995; Estrada et al., 1999). In the North Atlantic, the inflow of nutrients brought to the surface has also been mainly attributed to the vertical diffusion from deeper waters (Menzel and Ryther, 1960, 1961; Denman and Gargett, 1983; McGillicuddy and Robinson, 1997). In the subtropical NE Atlantic, the inter-annual variability of primary production has been also associated to both persistent and intermittent density fronts (Owen, 1981; Marañón et al., 2000).

In the last decades, numerical simulations have been gaining strong interest since they provide a relevant support to field measurements and satellite observations of primary production and biogeochemical properties of marine environments (Morel and André, 1991; Skogen et al., 1995; Aufdenkampe et al., 2002). Former numerical simulations lacked in coupling physical, biological and chemical processes (Steele, 1977; Denman and Platt, 1977; Kiefer and Kremer, 1981). However, combined studies were rapidly increasing thus providing suitable basis to the modelling of the ecosystem properties and evolution. Current ecological models operate at several time scales ranging from hours to years. For example, Sharples et al. (2001) used a model to evaluate hourly events affecting primary production in the thermocline. Cruzado (1982), Varela et al. (1992, 1994) and Zakardjian and Prieur (1998), among others, have focussed their modelling on the primary production at longer seasonal scales. The simulation of the pelagic ecosystem all the year over has also been gaining strong interest allowing to estimate organic and inorganic matter fluxes and budgets (e.g. Evans and Parslow, 1985; Doney et al., 1996; Oguz et al., 1996; Levy et al., 1998; Sharples, 1999).

One of the issues tackled by numerical models is the assessment of nitrogen fluxes, particularly nitrate associated with new primary production. Estimates of nitrate fluxes in oligotrophic ecosystems widely vary according to the place and methods. In the Sargasso Sea, using the Fasham et al. (1990) model (FDM), the nitrate flux in the upper mixing layer of water was estimated to range from 0.40 to 0.72 mol m^{-2} per year. Jenkins (1988) and McGillicuddy and Robinson (1997) have given estimates from ecological models within the same range. Doney et al. (1996) calculated the upward nitrate flux at 300 m depth to be 0.06 mol N m^{-2} per year similar to the value 0.072 mol N m^{-2} per year estimated by Gruber and Sarmiento (1997). In northwestern Mediterranean, the nitrate entering the upper water layers fuelling new primary production has been estimated with the use of vertically resolved ecological models in the range between 0.26 and 0.64 mol N m^{-2} per year (Tusseau et al., 1997; Levy et al., 1998).

The present paper is focussed on the ecological comparison of two oligotrophic environments with emphasis in nitrogen fluxes and primary production. This study was carried out using a one-dimensional vertically resolved model, which allows assessing the effect of different supply of nitrogen and irradiance affecting the phytoplankton primary production and the zooplankton secondary production. The turbulent environment in the model is assumed to depend on density also affecting the nitrogen flow and the interaction among biological communities. The selected environments were located at different latitudes in the Catalan Sea (NW Mediterranean) and in the subtropical northeast Atlantic Ocean. Since the nutrient flux estimates with the model depend on an adequate parameterisation of the physical properties and biogeochemical processes in the ecosystem, this paper first describes how the proposed model fits field observations and then investigates about fluxes in the water column and primary production.

2. Methods

2.1. The physical model

An improved version of the one-dimensional model described by Varela et al. (1992) thought to simulate the depth of chlorophyll maximum (DCM) during

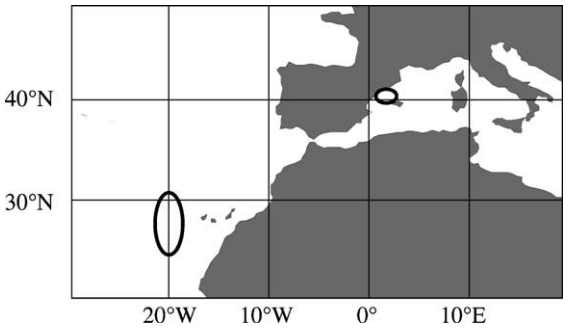

Fig. 1. Location of selected oceanographic stations in the Catalan Sea (vertical oval) and subtropical NE Atlantic (horizontal oval).

summer time, is used to simulate the temporal evolution (hourly steps) along the whole year of physical and biogeochemical variables in two open ocean stations. Temperature, salinity, density and irradiance are the physical variables interacting with inorganic nutrients (nitrate, nitrite and ammonium) and with phytoplankton and zooplankton as biogeochemical variables. The two selected oceanographic stations were located in the central Catalan Sea (CS), NW Mediterranean, and in the subtropical NE Atlantic (NEA) ocean (Fig. 1). The physical processes in the model force the state variables along 100 boxes arranged in the vertical dimension, each 3 m thick thus covering the upper 300 m depth of the water column, as schematically represented in Fig. 2. The rates of change were evaluated at 60 min time-step. All variables were subject to a vertical advection and vertical turbulent diffusion maintaining the mass-conservation principle.

Validation of the model results was carried out using historical field data of various cruises that took place in selected stations, obtained by staff from the Centre d'Estudis Avançats de Blanes (CEAB), Spain. Ninety-eight stations from the Catalan Sea between 40–41°N and 1–3°E, and 12 stations from the subtropical NE Atlantic between 20–24°E and 25–30°N were selected. The CS stations covered all seasons in the period 1985–1999 while the NEA stations covered only winter 1991 and summer 1992. In absence of real time series, historical temperature, salinity, chlorophyll *a*, nitrate and nitrite data, were grouped by seasons and integrated at various depths in order to be compared with seasonally integrated results generated by the present model.

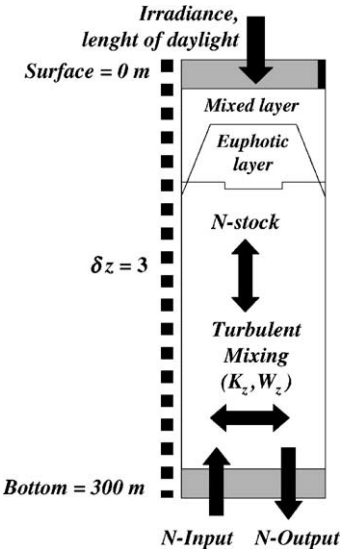

Fig. 2. Diagram of the numerical grid used in the model. The mixed layer cross down the euphotic layer in autumn and winter but it keeps above the euphotic layer during spring and summer times. Black block above to the right denotes lateral advection allowed compensating the upward advection.

The relatively low historical variability of temperature (°C) and salinity (psu) at 300 m depth led to fix the values for these variables in the bottom boundary of the model. Temporal evolution of temperature and salinity, imposed to the surface boundary as a sinusoidal function, was parameterised according to basic statistics (*mean* and *amplitude*) of historical data sets (Table 1). *B* represents temperature (°C) or salinity

Table 1
Basic statistics of surface and bottom (300 m depth) temperature and salinity in the selected environments, as deduced from the historical database

	Catalan Sea		Subtropical NE Atlantic	
	Mean	Amplitude	Mean	Amplitude
Upper boundary				
Temperature	17.9	±5.0	21.0	±3.0
Salinity	37.9	±0.3	37.0	±0.4
	Fix value		Fix value	
Bottom boundary				
Temperature	13.1		16.0	
Salinity	38.45		36.0	

(psu) and *phase* depends on the form of the sinusoid in the equation:

$$B = \text{mean} + \text{amplitude} \times \sin\left(\frac{2\pi}{365 - \text{phase}}\right) \quad (1)$$

2.1.1. Length of daylight (L_1)

The latitude of the stations and the Julian day control the length of daylight in hours computed following Brock (1981):

$$L_1 = 2W_1 \times \frac{180}{15\pi} \quad (2)$$

$$W_1 = \arccos\left\{-\tan(L)\frac{\pi}{180} \times \tan(D_1)\frac{\pi}{180}\right\} \quad (3)$$

$$D_1 = 23.54 \sin\left[\frac{2\pi(284 + N)}{365}\right] \quad (4)$$

where W_1 (°) is the angle hour, L is latitude assumed as 40.25°N and 27.5°N for the CS and NEA sites, respectively; D_1 is the declination of Earth, i.e. the angular distance at solar noon between the sun and the Equator; N is the number of days after 22 December. Results of the yearly daylight simulation are shown in Fig. 3, on the left.

2.1.2. Photosynthetic available radiation (PAR)

Total surface incident irradiance was assumed to be dependent on Astronomy, that is, the height of the Sun's plane over the horizon (computed daily) and the height of the Sun over the horizon (computed hourly). Both functions were simulated by trigonometric functions (Eqs. (5) and (6)). A constant fraction of the total irradiance (0.45) was assumed to be PAR (Baker and Frouin, 1987) (Fig. 3, right). Exponential extinction of PAR flowing through the water column depended on absorption and dispersion by the water and on the self-shading effect by phytoplankton (Eq. (7)).

$$\text{PAR}(0) = P_0 + P_1 \sin\left(2\pi\frac{N}{365}\right) \quad (5)$$

$$\text{PAR}(0, t) = \text{PAR}(0)\left\{1 + \cos\left[2\pi\left(\frac{t + L_1 - 12}{L_1}\right)\right]\right\} \quad (6)$$

$$\text{PAR}(i, t) = \text{PAR}(i - 1, t)\exp[-(k_w + k_c \times \text{PHY}(i) \times D_z)] \quad (7)$$

where P_0 is the annual mean value of PAR in surface assumed to be 180 and 250 W m^{-2} in the CS and NEA sites, respectively, P_1 is the amplitude of PAR here assumed as ±100 and 160, respectively, t is the time-step, L_1 is the length of daylight obtained from Eq. (2), k_w is the coefficient of vertical light attenuation due to pure water only (assumed as 0.06 m^{-1}), k_c is the constant for phytoplankton self-shading (assumed as 0.03 m^2 (mmol N)$^{-1}$), PHY(i) is the phytoplankton biomass at box i and D_z is the grid vertical resolution (3 m).

2.1.3. Turbulent environment

Based on theoretical simulations, Zakardjian and Prieur (1998) found the vertical advection should be lower than 2 m per day in or near geostrophic fronts in the northwestern Mediterranean to explain the summer

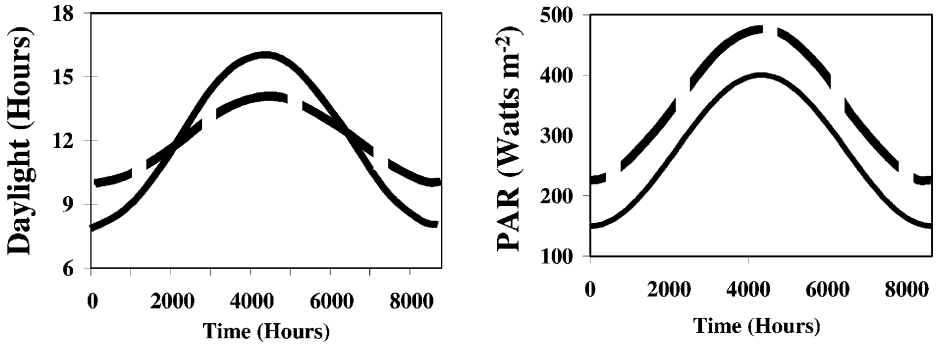

Fig. 3. Time series of calculated length of daylight and surface PAR in the Catalan Sea (solid lines) and the subtropical NE Atlantic (long-dashed lines).

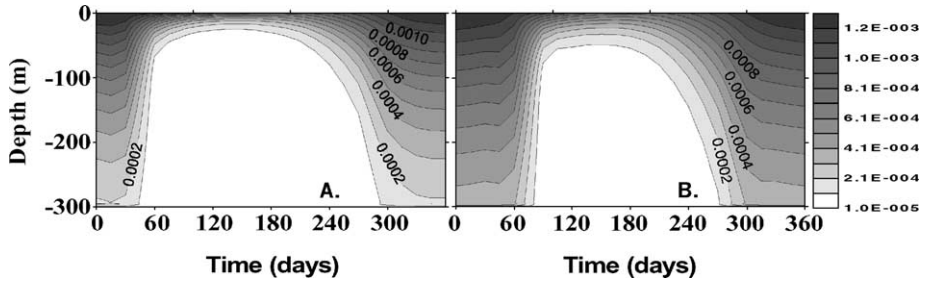

Fig. 4. Time series of simulated vertical turbulent diffusion (K_z in $m^2\,s^{-1}$) (A) in the Catalan Sea and (B) the subtropical NE Atlantic.

vertical distribution of primary production. Sensitivity tests with the present model gave a much lower constant value of 0.05 m per day for the whole year allowing a proper seasonal distribution of chlorophyll *a* concentration in the water column. Higher velocities produced non-realistic values of all state variables close to the surface. In keeping continuity, we assumed the upwelled flow to escape laterally from the upper box.

Vertical eddy diffusivity (K_z) calculated from the density field according to Osborn (1980):

$$K_{(z)} = \frac{0.25\varepsilon_{(z)}}{N^2_{(z)}} \tag{8}$$

$$N^2_{(z)} = -\frac{g}{\rho_w} \times \frac{\partial \rho}{\partial_z} \tag{9}$$

where $\varepsilon_{(z)}$ is the turbulent kinetic energy (TKE) dissipation rate at a given depth z ($m^{-2}\,s^{-3}$). TKE was assumed constant in the mixing layer ($\varepsilon = 1E{-}02$) but exponentially decreasing below it until reaching a background value of $\varepsilon = 1E{-}08$. $N_{(z)}$ represents the Brunt–Väisälä buoyancy frequency (s^{-1}), g is acceleration due to gravity ($g = 9.82\,m\,s^{-2}$), ρ_w was calculated according to Millero and Poisson (1981) equations.

The simulation results of the eddy diffusivity of the model are shown in Fig. 4. Parameterisation of the eddy diffusivity yielded values from a background value of 0.1–13.0 $cm^2\,s^{-1}$ in the mixing layer, in the range of estimates from literature. Lewis et al. (1986) found a diffusivity of 0.1–1.0 $cm^2\,s^{-1}$ explaining nitrogen fluxes in the subtropical NE Atlantic. Doney et al. (1996) used a background diffusion of 0.1 $cm^2\,s^{-1}$ in the modelling of a station close to Bermuda. Zakardjian and Prieur (1998) studied primary production in the Western Mediterranean using the Osborn (1980) parameterisation yielding a diffusion distribution pattern and magnitude in the vertical similar to our estimates. The Ligurian Sea primary production was successfully modelled used a range of 0.0017–3 $cm^2\,s^{-1}$ turbulent diffusion (Tusseau et al., 1997).

A sensitivity test of the model allowed determining the lower limit of the mixing layer that reasonably matched the mixing layer from literature. The lower limit of the mixing layer was defined as the depth at which the density difference in respect to the surface is 0.32 and 0.21 $g\,kg^{-1}$ in the CS and NEA, respectively. Nevertheless, when these lower limits in autumn and spring times were deeper than 150 and 200 m in the CS and NEA, the sigma–theta difference in respect to the surface was set to 0.0003 $g\,kg^{-1}$. The greater diffusion values are calculated in the mixing layer (>1 $cm^2\,s^{-1}$) and the lower values were found around stronger vertical sigma–theta gradients. When sigma–theta ρ in a box i was greater than that just below it (plus $\delta = 0.00001$), overturning was applied to all state variables (k) as follows:

$$\text{If } \rho_{i-l} > \rho_i + \delta, \quad \text{then} \begin{cases} X(k,i) = \dfrac{X(k,i) + X(k,i-1)}{2} \\ X(k,i-1) = X(k,i) \end{cases} \tag{10}$$

Since overturning was not enough to explain the formation of the near surface phytoplankton bloom occurring in late winter and early spring, convection was forced on the tenth day at the beginning of the year on all state variables along the entire mixing layer. This favoured both a faster upwelling of nutrients

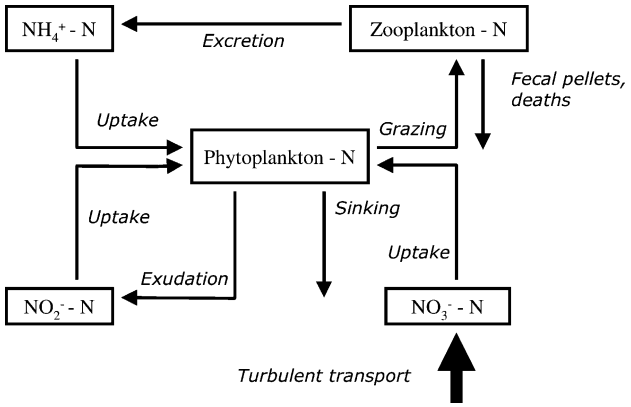

Fig. 5. Pathways of the simulated nitrogen flow in upper water layers of the selected ecosystems.

from deeper waters and the homogenisation of the state variables in the water column. The realistic character of convection is supported in the CS where it is known to affect the water column in January–February during deep-water formation (Levy et al., 1998). In the Sargasso Sea (also in the subtropical North Atlantic), convection reaching 250 m depth has been reported at the end of February (Hurtt and Armstrong, 1996).

2.2. The biogeochemical model

The model assesses nitrogen flowing through five compartments or state variables in the pelagic environment, as shown in Fig. 5. Dissolved nitrite (NO_2^-), nitrate (NO_3^-) and ammonium (NH_4^+) are nutrients taken up by a phytoplankton community, in turn, being grazed by a zooplankton community. Zooplankton forces both recycling of ammonium and non-recycling material. The best fitting coefficients and parameters for the functions are shown in Table 2.

The evolution of nitrate, nitrite and ammonium was similarly formulated as shown for the nitrate (NO_3) case:

$$\frac{\partial \mathrm{NO_3}}{\partial t} = \frac{\partial}{\partial z}\left(K_z \frac{\partial \mathrm{NO_3}}{\partial z}\right) - w\left(\frac{\partial \mathrm{NO_3}}{\partial z}\right) - (U_{\mathrm{NO_3}} \times \mathrm{PHY}) \quad (11)$$

Table 2
Values given to fitting parameters and coefficients in both selected environments as deduced from the sensitivity of the model

Symbol	Value	Definition	Units
K_{NO_3}	0.9	Half-saturation constant for nitrate uptake	mmol N m^{-3}
K_{NO_2}	0.8	Half-saturation constant for nitrite uptake	mmol N m^{-3}
K_{NH4}	0.7	Half-saturation constant for ammonium uptake	mmol N m^{-3}
ψ	1.5	Ammonium inhibition parameter for nitrate and nitrite uptake	mmol N m^{-3}
γ	2.5	Phytoplankton exudation fraction of nitrite	%
V_{PHY}	3.0	Phytoplankton maximum growth rate	per day
μ	0.1	Zooplankton mortality rate	per day
ε	80	Ammonium fraction of zooplankton excretion	%
Ω	20	Faecal pellets fraction of zooplankton excretion (detrital)	%
λ	30	Zooplankton assimilation efficiency	%
K_g	1.68	Zooplankton half-saturation for ingestion	mmol N m^{-3}
I_{max}	1.2	Zooplankton maximum ingestion rate	per day

The uptake of nitrate, nitrite and ammonium by phytoplankton cells is based on the Michaelis–Menten formulation:

$$U_{NO_3} = V_{PHY}\left(\frac{NO_3}{K_{NO_3} + NO_3}\right) e^{-\psi(NH_4)} \quad (12)$$

where V_{PHY} is phytoplankton maximum growth rate and K is the half-saturation constant for nitrate. The exponential function represents the suppression of nitrate uptake by ammonium. ψ is the ammonium inhibition parameter for nitrate and nitrite uptake.

A fraction of the nitrate (γ) taken up during the light hours by phytoplankton is exuded in the dark as nitrite (PHY_{EXU}):

$$\text{If } PAR(i,t) < PAR_{surface} \times 0.1,$$
$$\text{then } PHY_{EXU} = \gamma \times U_{NO_3} \times PHY \quad (13)$$

The biological processes involved in equations describing the nitrite and ammonium evolution are $(PHY_{EXU} - U_{NO_2} \times PHY)$ and $(\varepsilon - U_{NH_4} \times PHY)$, respectively, where ε represents the fraction of nitrogen ingested by zooplankton that is excreted (Eq. (19)).

Limitation of phytoplankton growth by PAR or by nutrients follows the Liebig's law of minimum. This means that the first resource to be depleted at a given time and depth in the water column (PAR/nutrients) limits the phytoplankton growth. Phytoplankton growth (nutrient uptake) limitation by light is formulated as described by Varela et al. (1992):

$$U_{PAR} = V_{PHY} \times \frac{PAR_{(z,t)}}{K_{PAR} + PAR(z,t)} \quad (14)$$

where K_{PAR} is the half-saturation constant of PAR (here assumed to be $20\,W\,m^{-2}$). The proportion of each nutrient to be taken up (U) under light limitation when $U_{PAR} < U_{NO_3} + U_{NO_2} + U_{NH_4}$, is computed as:

$$U = U_{PAR} \times \frac{U_X}{U_{NO_3} + U_{NO_2} + U_{NH_4}},$$
$$\text{for } U_X = U_{NO_3} \text{ or } U_{NO_2} \text{ or } U_{NH_4} \quad (15)$$

A chlorophyll-to-nitrogen ratio taken as $1\,mg\,Chl\,(mmol\,N)^{-1}$ (Marra et al., 1990) was used to compare field chlorophyll observations with N-phytoplankton model results. The phytoplankton equation (PHY) includes w_s as the settling velocity ($w_s = -0.03\,m$ per day), and G as the phytoplankton grazing by zooplankton (Eq. (20)).

$$\frac{\partial PHY}{\partial t} = \frac{\partial}{\partial z}\left(K_z \frac{\partial PHY}{\partial z}\right) - (w + w_s)\frac{\partial PHY}{\partial z} + PHY(U_{NO3} + U_{NO2} + U_{NH4}) - PHY_{EXU} - G \quad (16)$$

The evolution equation of zooplankton was formulated to have the following biological term: $(\lambda \times G - M - \varepsilon - \Omega)$, λ being the zooplankton assimilation efficiency, M representing the zooplankton mortality (Eq. (18)), and Ω is the zooplankton faecal pellet production (Eq. (20)).

$$G = I_{max}[ZOO] \times \left(\frac{PHY}{K_g + PHY}\right) \quad (17)$$

$$M = \mu \times [ZOO]^2 \quad (18)$$

$$\varepsilon = G(1-\lambda) \times 0.25 \quad (19)$$

$$\Omega = G(1-\lambda) \times 0.75 \quad (20)$$

where I_{max} is the maximum ingestion rate and K_g is the half-saturation constant for ingestion. μ is the zooplankton mortality rate multiplied by a quadratic function of the zooplankton biomass. This could be interpreted as either cannibalism within the zooplankton compartment or by another predator whose biomass is proportional to that of the zooplankton (Edwards and Yool, 2000). A sensitivity test of the model supported this parameterisation of zooplankton mortality since it yielded the best results for the zooplankton stocks. By using a similar parameterisation, Evans (1999) found similar effects on zooplankton with the FDM model.

Standard initial conditions for temperature, salinity, nitrate, nitrite, ammonium, chlorophyll and zooplankton concentrations were obtained after 6 years of simulation with arbitrary initial conditions and perpetual year driving forces. This length of time was necessary to make inter-annual variability smaller than 1% assuming a quasi steady state.

2.3. Estimates of nitrogen fluxes and primary production

At the lower boundary of the model (300 m depth), a relatively low variability of nutrient concentrations

is observed from historical database, with nitrate concentrations close to 8 and 4 mmol m^{-3} in the CS and NEA sites, respectively. This led to fix these values for the nitrate variable in the bottom, where vertical diffusion allows gains and losses of matter (depending on its concentration gradient) while advection produces gains or losses of matter depending on its concentration. The flow of nitrogen was treated as a scalar magnitude (mmol N m^{-3} s^{-1}). The model allowed assessing the upward flux of nitrate from the water below the euphotic zone and the internal fluxes through the biogeochemical compartments. In determining the total upward flux of nitrogen (μmol m^{-2} s^{-1}) at such depths the diffusive flux (K_z) was added to the advective flux term (w)

$$\text{nitrate flux} = wN + K_z \left(\frac{\partial N}{\partial z} \right) \quad (21)$$

Primary production, the rate of inorganic carbon incorporated to the phytoplankton biomass, was estimated using a Redfield C:N ratio of 6.625. New production in the model was assumed as that originated by the uptake of nitrate flowing from the bottom boundary of the model domain. The production derived from the ammonium uptake was assumed as regenerated production.

3. Results

3.1. Depth and time evolution of modelled physical properties

Simulations of temperature, salinity and σ_θ in depth and time in the upper water layers of both the CS and the NEA are shown in Fig. 6. Expected surface summer temperature maxima contrasted with the minimum surface values in wintertime (Fig. 6, top). The 15 °C isotherm was observed at approximately 80 m depth during spring and summer in the CS while in autumn it sank to about 120 m depth. This isotherm disappeared during late spring and winter due to the homogenisation forced in the mixing layer by the vertical convection making temperature to be 13.6 ± 0.6 °C along the entire water column. The 19 °C isotherm in the NEA was observed at ∼100 m depth showing a similar temporal distribution pattern than the 15 °C isotherm in the CS. The summer thermocline in the CS was shallower and thinner (between ∼30 and 50 m depth) than in the NEA (between ∼40 and 90 m depth). The vertical gradient of temperature above thermocline in the CS was twice the gradient in the NEA station (0.09 and 0.05 °C m^{-1}, respectively). Just the opposite occurred below the thermocline, with a temperature gradient in the former site being half of that observed in the latter site (0.01 and 0.02 °C m^{-1}, respectively), suggesting a more homogeneous water column in the CS than in NEA.

Regional differences of the physical properties in both environments are better shown in salinity (Fig. 6, middle) than in temperature. At surface, in the CS, the lowest salinity value was modelled in summer while the highest value appeared in late autumn and winter. Just the opposite occurred in the NEA site, where the highest value was found in summer and the minimum in late autumn and winter. Temperature decreases with depth in both stations while salinity increases toward the bottom in the CS but decreases in NEA. A diffuse halocline was observed in the CS between ∼60 and 80 m depth while in the NEA station halocline is absent. The vertical gradients of salinity were similar in both cases being 0.002 and 0.003 m^{-1} in the CS and NEA.

In spite of the differing vertical distribution patterns of salinity, σ_θ kept mainly governed by temperature in both sites (Fig. 6, bottom). A pycnocline parallel to thermocline was found in summertime in the CS between ∼30 and 50 m depth, while in the NEA case it was rather diffuse between ∼30 and 100 m depth. Above the pycnocline, the gradients in the CS case were stronger, around 2.8 kg m^{-4} while in the latter, they were around 1.2 kg m^{-4}. The higher the density gradients, the smaller the turbulent diffusion (see Fig. 4) and the nitrogen transport. Almost all year round, except in the early winter and late autumn, σ_θ of decreased ∼2 kg m^{-3} in the first 100 m in both environments. Below this depth, no strong differences of σ_θ were observed.

3.2. Depth and time evolution of modelled biogeochemical properties

The annual cycle of modelled biogeochemical variables is shown in Fig. 7. The typical situation of high nitrate depletion in surface waters particularly in

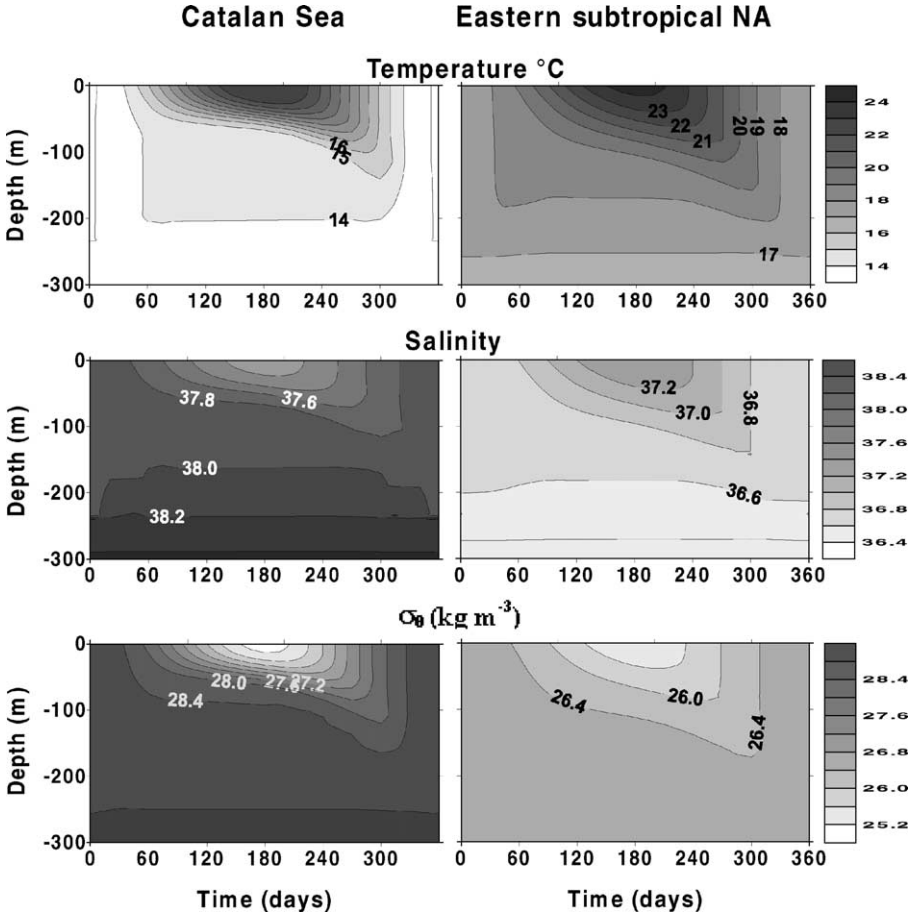

Fig. 6. Idealised time series of temperature, salinity and σ_θ by the model.

summer is common to the CS and NEA. In the early winter, the nitrate concentration is relatively high in surface due to the vertical convection of the mixing layer. This makes the values of nitrate at the beginning of the year around 1.5 and 0.5 mmol m^{-3} in the CS and NEA, respectively. This nitrate concentrations cause phytoplankton blooms to take place just near the surface at late winter. The blooming phytoplankton rapidly depletes nitrate in the surface layer that stays this way up to the late autumn when a weak upwelling of nitrate from intermediate waters is observed going up to the subsurface as a consequence of the thickening of the mixing layer after summer stratification is over. Since nitrate concentration in the bottom boundary was twice as much in the CS than in NEA, below thermocline higher nitrate gradients were found in the former case than in the latter (0.03 and 0.02 mmol m^{-4}, respectively).

The thickness of nutrient-depleted surface water layer was higher in the NEA site than in the CS, strongly dependent on the phytoplankton uptake. First, the phytoplankton uptake covered a wider layer of water in the NEA case than in the CS. The nitrate values linked with subthermocline water correspond to the nitrate isolines 1.0 and 0.5 mmol m^{-3} in the CS and the NEA, shallower in the former (∼80 m) than in the latter (∼100–120 m).

The relatively low amount of nitrate transported upward to the euphotic zone from the bottom boundary in the NEA site in comparison with that in the CS, was considered as a limiting factor for the phytoplankton stock. In fact, chlorophyll *a* concentration

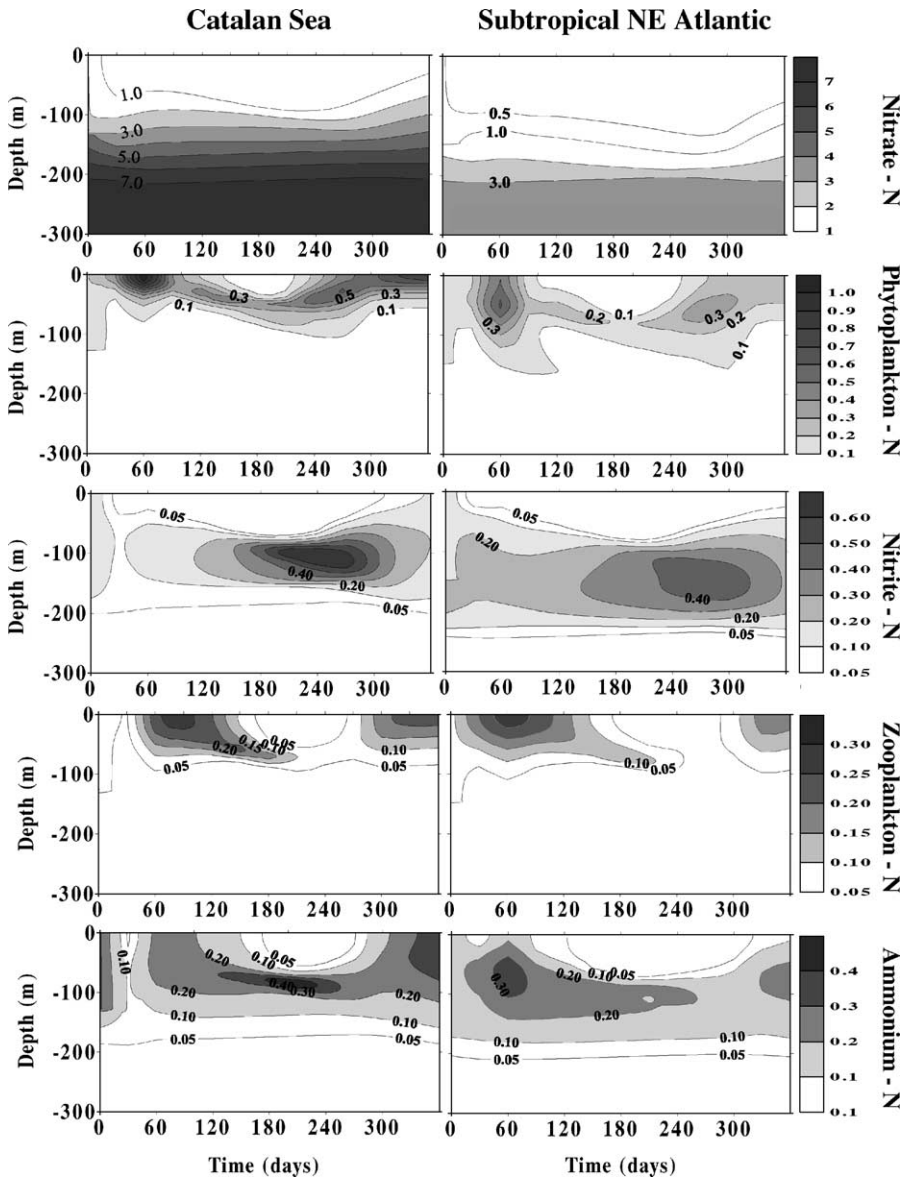

Fig. 7. Simulated time series of biological and chemical state variables in the selected oligotrophic environments (mmol m^{-3}).

in NEA was around half of that in CS. In late winter, a phytoplankton bloom appeared with a maximum around 0.6 mmol m^{-3} close to the surface in the CS and 1.1 mmol m^{-3} at about 40 m depth in NEA. These values contrasted with a surface minimum in summer lower that 0.5 mmol m^{-3} in both stations. Another feature common to both environments was the surface chlorophyll increasing in late summer and autumn forced by the weakening in daily irradiance and increasing in mixing layer depth (and vertical convection) that favoured at the same time, the increase of nitrate concentrations in the upper water layers. This second phytoplankton bloom never reached the maximum values observed in the late-winter/spring bloom.

Along the year, a persistent layer of water with chlorophyll concentration higher than 0.1 mmol m^{-3}

was observed in both environments. In general, this layer was thicker and deeper in NEA than in the CS. At the early spring, 0.1 mmol m^{-3} chlorophyll phytoplankton reaches the surface in both case studies. The lower limit of this chlorophyll layer was variable, having an average of 75 ± 25 m depth in the CS and 115 ± 40 m in NEA. Summer phytoplankton maximum was about 40 m deeper in NEA than in the CS sites, looking for the nutrients that were scarcer in the upper layers. This was possible due to the high surface irradiance making the euphotic zone wider and allowing active phytoplankton to sink deeper in NEA. The increasing of nutrients in the euphotic zone has been observed to increase the phytoplankton biomass rather than increasing the growth rates, as observed in the Sargasso Sea (Goericke and Welschmeyer, 1998; Morel et al., 1993). In the present modelling, the role of the nutrient enrichment by vertical mixing during winter coincides with the phytoplankton biomass (standing stock) increasing.

As occurred with nitrate, nitrite was highly depleted at the surface almost all year round due to the high rate of phytoplankton uptake of nitrate after the late winter bloom. The nitrite maximum with concentrations higher that 0.1 mmol m^{-3} was generally found beneath the chlorophyll *a* layer. The average depth of such a maximum was 90 and 140 m in the CS and NEA, respectively. The maxima were observed in late summer (0.61 and 0.4 mmol m^{-3}, respectively) after the weakening of the subsurface chlorophyll maximum and before it began raising upward in autumn. This nitrite maximum had a lag with regard to the formation of the DCM between 60 and 90 days in both stations.

Gains and losses of zooplankton were parameterised by equations that forced a standing stock less variable in time in respect of the phytoplankton standing stock. In general, a layer of maximum zooplankton density was observed following the phytoplankton maximum. This made that zooplankton showed two maxima, as for phytoplankton, localised close to the surface in late winter and autumn. A considerable reduction of surface zooplankton biomass took place after the water column was homogenised in winter. Nevertheless, a layer with zooplankton biomass above 0.05 mmol m^{-3} was continuously kept around the year, also contributing to increase the ammonium concentration. During summer, the CS held the highest concentration of ammonium, particularly at depths lower than the DCM, as the balance between the excretion by zooplankton and consumption by phytoplankton favoured the former process.

4. Discussion

4.1. Validation of physical properties

The physical parameterisation in the present model reasonably forces the dynamic of processes taking place into and below the mixing layer. More sophisticated parameterisation like the Mellor–Yamada 2.5 turbulence closure scheme is often referred to as a good tool describing biogeochemical processes in the mixing layer (Chen and Annan, 2000). Nevertheless, other studies point to the vertically resolved models as highly efficient simulating observations in upper water layers with similar results as those given by the Mellor–Yamada parameterisation (Oguz et al., 2001). The ecological model used in the present work is not compared with other turbulence schemes. However, the results obtained with the parameterisation made in this work are reliable at monthly and seasonal scales as the model reasonably reproduced observed features in the pelagic ecosystems (Figs. 8 and 9).

Even though the satisfactory general results, some differences between field observations and model estimates were found. With respect to temperature (Fig. 8, top), the most important differences between field and model results are found in autumn, when simulation underestimated surface temperature by about 2 °C. Temperature observed, remained relatively homogeneous below ~100 m depth at all seasons while the model profiles tend to be more variable and in general, higher than observations. This suggest a relatively high eddy diffusion below ~100 m depth increasing more than expected the temperature and also altering the vertical distribution of all the state variables as shown further on.

As occurs with temperature, salinity in the CS shows some non-significant differences with field observations (Fig. 8, bottom). The summer halocline in the model simulations does not appear to be very realistic, since in the field data, salinity shows only a small but constant downward gradient along the entire water column. We attributed this to the relatively high turbulent diffusion in the model below ~100 m depth.

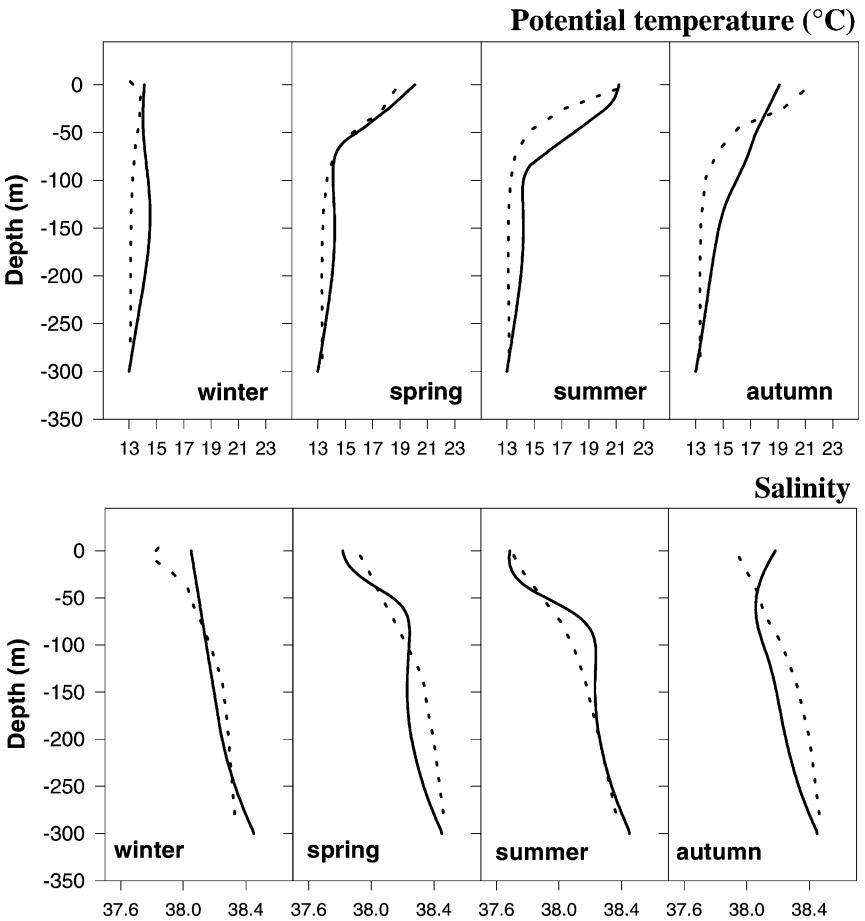

Fig. 8. Comparison of seasonal means of potential temperature and salinity simulated (solid lines) with field observations (dotted lines) in the Catalan Sea case study.

Surface salinity was overestimated in winter and autumn by near 0.2 psu. In the NEA case, the model fits better with field observations the averaged temperature and salinity for winter and summer (Fig. 9). The success in this modelling could not be corroborated for the other seasons due to the lack of field data.

4.2. Validation of biogeochemical properties

The comparison of the seasonal means of simulated nitrate with observations shows a high similarity for the CS case (Fig. 10, top). The model smoothes the observed spring variability of nitrate below ∼100 m depth, contrasting with a good match found between model and observations in autumn. In the case of chlorophyll *a* (Fig. 10, bottom), at depths greater than ∼60 m, the model underestimated chlorophyll *a* by about 0.1 mg m^{-3}. The phytoplankton stock was limited by the difference in the amount of nitrate transported from the bottom boundary in comparison with NEA, since in the CS the nitrate concentration was twice that in NEA. However, the phytoplankton growth below ∼60 m depth appears to be light rather than by nitrate limited. In the CS simulation, the summer DCM was around 60 m depth, while the field data suggested an average maximum at 75 m depth. In the model, phytoplankton rapidly diminished below the DCM, reaching the lowest value at about 100 m depth. On the contrary, the field data suggest a high phytoplankton concentration below

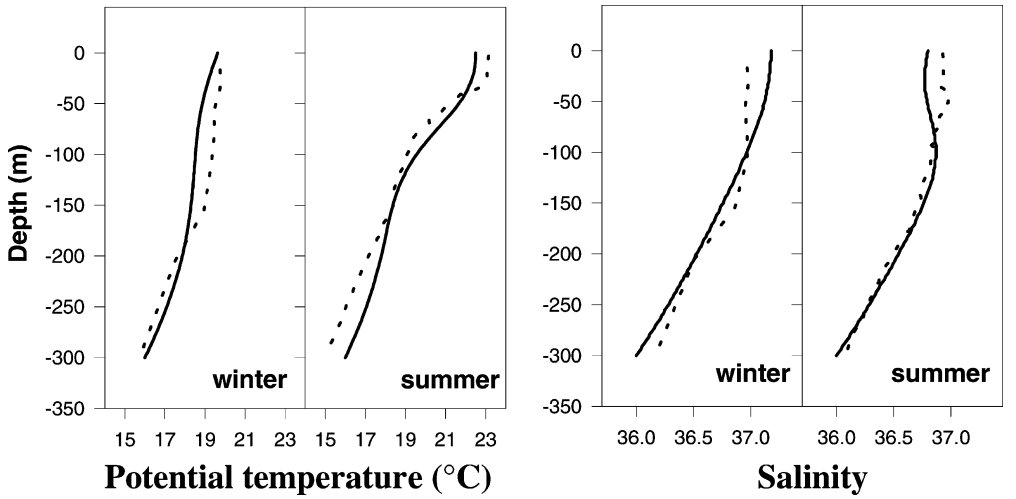

Fig. 9. Comparison of seasonal means of potential temperature and salinity simulated (solid lines) with field observations (dotted lines) during winter and summer seasons, in the subtropical NE Atlantic case study.

DCM that decreased linearly until about 140 m depth. DCM was found within the depth range given by other authors. Pedrós-Alió et al. (1999) and Estrada (1985) observed DCM in the NW Mediterranean at 40–80 m depth. Irradiance in the modelled DCM was about 0.5% that in surface in agreement with previous work carried out in the same area (Morel et al., 1993; Varela et al., 1994). Chlorophyll maximum in the CS (1.1 mmol m^{-3}) was in the range of historical observations (Cruzado and Kelley, 1974; Estrada et al., 1999). Model results and observations also show that DCM is closely associated with the nitracline, as previously observed in the same area (Velásquez, 1997).

Validation of nitrate and chlorophyll *a* during summer in NEA is shown in Fig. 11. A layer of nitrate-depleted surface waters appears reaching a bottom boundary of 90 m depth in the model, while in the field data it was 30 m deeper. Nitrate in the model was around 1 mmol nitrate per m^3 higher than observations around 90–150 m depth, coinciding with underestimating of the modelled chlorophyll *a* concentration at same depths. As occurred in the CS, chlorophyll *a* observations beneath DCM were higher than the estimates given by the model, thus reaffirming that the phytoplankton stock in the model at the depth of the chlorophyll maximum could be light rather than by nitrate limited. Field data and model results show the summer DCM to be closer to the nitracline, as previously observed (Herbland and Voituriez, 1979; Bahamón, 2002), also coinciding with the CS case study. Chlorophyll *a* maximum (0.6 mmol m^{-3}) was half the maximum modelled by Doney et al. (1996) in the Sargasso Sea, in general agreement with observations from JGOFS Bermuda Atlantic Time-Series Site. DCM was nevertheless, coinciding with previous values given by Bricaud et al. (1992) for the Sargasso Sea.

In the CS, nitrite was successfully simulated and validated with seasonal averages of field observations (Fig. 12). The main discrepancy was found during winter when nitrite was underestimated by about 0.1 mmol m^{-3} in the upper 50 m. The field data suggest that nitrite tends to accumulate in small amounts below 150 m. Bacterial oxidation of organic matter not being considered in our model could explain this event. The uptake of nitrite in the model was assumed to take place in the light hours in the euphotic layer while the nitrite exudation was assumed to take place at low radiation during the day and at night. This made the layer beneath the chlorophyll maximum a good place for the nitrite exudation favoured by the phytoplankton self-shading. Unfortunately, in the NEA case, no validation was carried out for the simulated data since field observations were not available from selected cruises to be compared.

Current models rarely simulate nitrite in relation to phytoplankton primary production. Vaccaro and Ryther (1960) early described the first nitrite

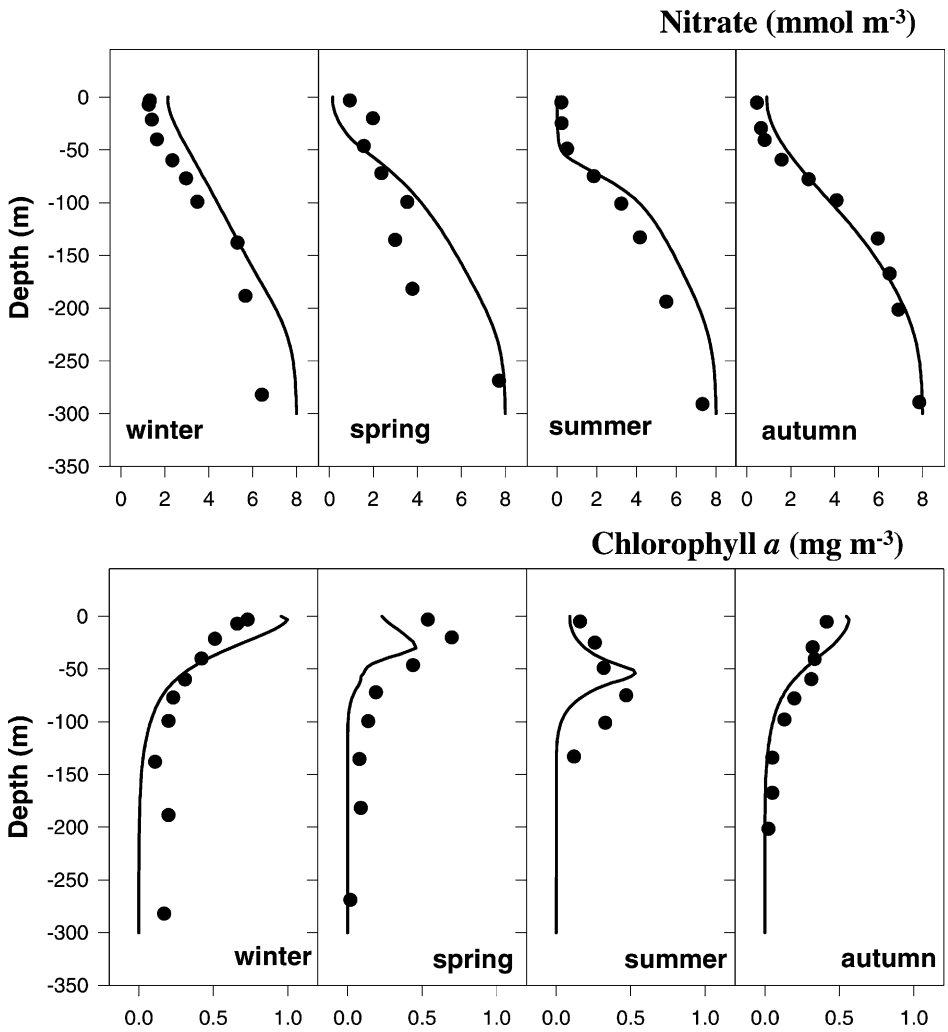

Fig. 10. Comparison of seasonal means of nitrate and chlorophyll *a* modelled (solid lines) with field observations (solid circles) in the Catalan Sea.

maximum above 200 m depth in oligotrophic areas including the Mediterranean Sea. This nitrite was considered to be the result of both bacterial ammonium oxidation and nitrate reduction by phytoplankton at low light levels (Carlucci et al., 1970; Raimbault, 1986). In our model we assumed the role of nitrate reduction by phytoplankton as the main source of nitrite, with bacterial nitrification as numerically negligible (Eppley and Peterson, 1979), that nevertheless could explain observed variations in the nitrate concentration below 150 m not found in the model. In the present study, highest concentrations of nitrite were located below the DCM, in close agreement with the field data and other related works reported for the Mediterranean Sea (Vaccaro and Ryther, 1960; Blasco, 1971). This validates the hypothesis that the nitrate reduction by phytoplankton in the dark could be responsible for most part of the nitrite maximum.

Summer zooplankton biomass estimated by the model (Fig. 7) at the maximum (0.05–0.10 mmol N m^{-3}) were in agreement with the data reported for the same area by Alcaraz (1988) who estimated the zooplankton in summer at about 0.06–0.08 mmol N m^{-3}. In the NEA site, such a layer was not continuous but broken

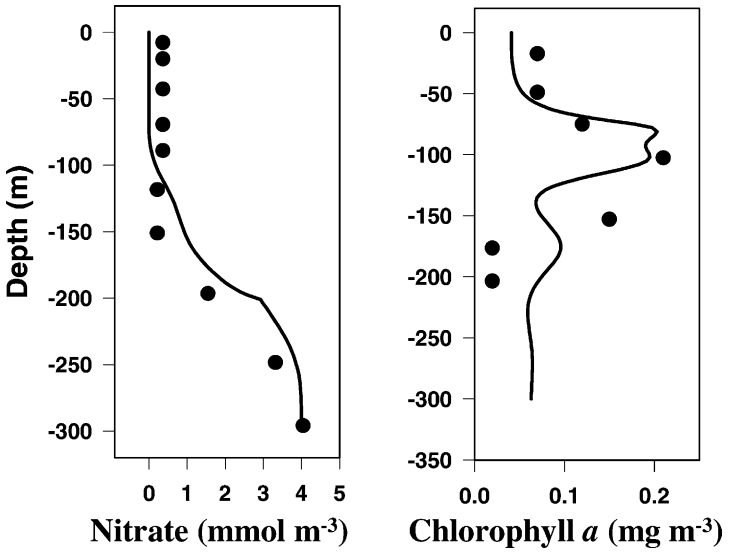

Fig. 11. Comparison of summer nitrate (left) and chlorophyll *a* (right) modelled (solid lines) with field observations (solid circles) in the subtropical NE Atlantic.

in the early autumn due to the relatively low phytoplankton availability that limited the sustainability of the zooplankton standing stock. At the middle of autumn when phytoplankton increased its biomass over 0.3 mmol m^{-3}, zooplankton biomass was also recovered, reaching concentrations above 0.05 mmol m^{-3}. The zooplankton maximum ingestion rate (I_{max}) was tested with values lower than the ones used in the model (1.2 per day). Higher values increased the zooplankton biomass, up to an order of magnitude, that produced a rapid reduction of the phytoplankton biomass. At the same time, this induced a high concentration of ammonia in the surface breaking the equilibrium in the nitrogen fluxes along the rest of compartments in the model. The best zooplankton mortality rate from the sensitivity test was 0.1 per day as shown in Table 2. Values lower than those made the model to become unstable, while higher

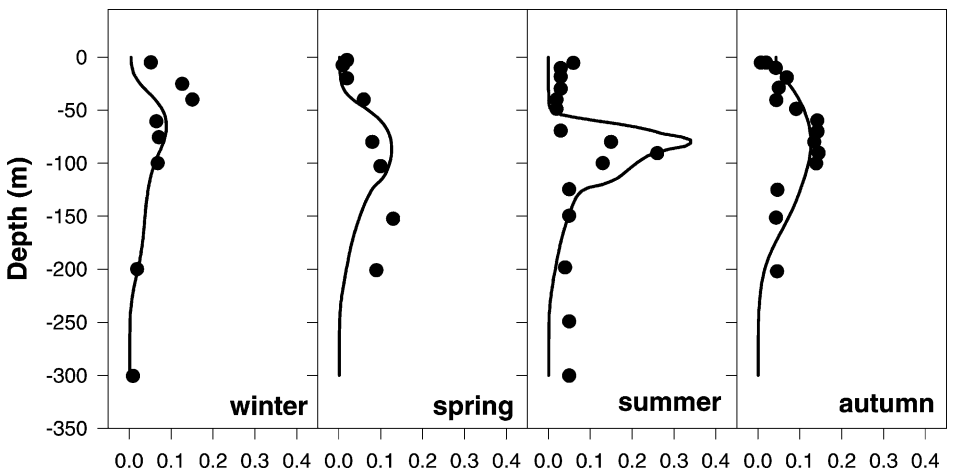

Fig. 12. Comparison of the seasonal means of nitrite simulated (solid lines) with field observations (solid circles) in the Catalan Sea case study.

Table 3
Estimates of nitrogen fluxes at several depths below the euphotic layer in the Catalan Sea (CS) and subtropical NE Atlantic (NEA)

Area	Depth (m)	Advective fluxes (μmol m^{-2} per day)	Diffusive fluxes (μmol m^{-2} per day)	Total fluxes	
				In μmol m^{-2} per day	In mol m^{-2} per year
CS	120–130	144	1632	1776	0.64
	190–200	298	140	438	0.16
	290–300	380	5	385	0.14
NEA	150–160	24	582	606	0.22
	190–200	120	197	317	0.11
	290–300	187	5	192	0.07

values forced a strong and unrealistic reduction of the zooplankton standing stock. In both environments, the zooplankton grazing controlled the phytoplankton bloom in wintertime, but it made the phytoplankton biomass to be reduced up to ~0.5 mmol m^{-3} in the CS and ~0.2 mmol m^{-3} in the NEA.

In the NW Mediterranean, Estrada (1985) found an ammonium maximum reaching about 0.3 mmol m^{-3} around the DCM that is in the lower limit of our model results (0.3–0.4 mmol m^{-3}, Fig. 7). Levy et al. (1998) found a similar vertical distribution of the ammonium concentration modelled in the Ligurian Sea (NW Mediterranean). In the present study, higher zooplankton stocks in the CS in comparison with NEA, explain higher ammonium concentrations with an ammonium excretion fraction assumed to be constant in both cases studied.

4.3. On the upward nitrogen fluxes and nitrogen stocks

A summary of the upward nitrogen fluxes toward the euphotic layer is shown in Table 3. At the range of 290–300 m depths, the diffusive–advective transfer of nitrate into the model domain was 0.39 and 0.19 mmol N m^{-2} per day in the CS and NEA, respectively. The nitrate transfer increases upwards with the increase of the vertical nitrate gradient. Following this trend, at 190–200 m depths, the total nitrate flux was a bit closer in both cases (0.44 and 0.32 mmol N m^{-2} per day in the CS and NEA). At 190–200 m depth ranges, the diffusive flux of nitrate was higher in NEA (0.20 mmol m^{-2} per day) than in the CS (0.14 mmol m^{-2} per day) due to a higher gradient induced by phytoplankton uptake at greater depths. Below the euphotic layers (~120–130 and 150–160 m in the CS and NEA cases, respectively), the total flux of nitrogen increased up to 1.78 and 0.61 mmol m^{-2} per day (equivalent to 0.64 and 0.22 mol N m^{-2} per year), respectively. The advective fluxes in both cases decreased upward with the nitrate concentration. The nitrate entering below the euphotic layer in the CS (0.64 mol N m^{-2} per year) matched quite well the estimated exported production of 0.7 mol N m^{-2} per year from the upper layer in the Ligurian Sea (Tusseau et al., 1997). Levy et al. (1998) calculated a vertical flux of nitrogen at 100 m depth in the Ligurian Sea of 0.26 mol N m^{-2} per year. The flux at 100 m depth in the Ligurian Sea is comparable with that found in the Catalan Sea in the range of 170–180 m depth.

The simulated nitrogen flux in NEA is within the range given for the western basin of the subtropical NA gyre. Doney et al. (1996), at a station close to Bermuda, gave an annual estimate of upward nutrient flux across the 300 m depth surface of 0.06 mol N m^{-2} per year closely matching our estimates at the same depth in the NEA site (0.07 mol N m^{-2} per year). The nitrogen flux estimated by Gruber and Sarmiento (1997) in the Sargasso Sea (0.072 mol N m^{-2} per year) was also coincident whit our estimate at 290–300 m depth, suggesting similarities in the amount of nitrogen required to sustain the low but continuous primary production. The estimated nitrate flux at the base of the euphotic layer (0.606 mmol m^{-2} per day) was somewhat lower than that given by Lewis et al. (1986) in the same area (0.807 mmol m^{-2} per day). Planas et al. (1999) give estimates of diffusive nitrate flux of 0.38 ± 18 mmol NO_3 m^{-2} per day in the central Atlantic, where thermocline is at the same depth of the nitracline. The maximum values of the latter estimates (0.56 mmol NO_3 m^{-2} per day) match our estimates of diffusive fluxes (0.58 mmol NO_3 m^{-2} per

day), even though our estimates are made along the nitracline that is below the thermocline.

The estimate of the nitrogen flux by the present model in NEA differs from field measurements by Jenkins (1988) who computed a flux of 0.6 ± 0.2 mol N m^{-2} per year (our estimate was 0.22 mol N m^{-2} per year) by using ^{3}He as a diffusion tracer along the thermocline. McGillicuddy and Robinson (1997), using a coupled physical–biological model, estimated the upward flux of nitrogen in the Sargasso Sea in 0.5 mol N m^{-2} per year. These estimates are close to that estimated by Fasham et al. (1990) using numerical simulation of the planktonic domain in the Sargasso Sea (0.56 ± 0.16 mol N m^{-2} per year). However, a further simplified version of the Fasham et al.'s model with a reduced number of parameters, resulted in lower estimates of the nitrogen flux of 0.2 mol N m^{-2} per year (Hurtt and Armstrong, 1996) matching our model results. Gnanadesikan et al. (2002) compared different ecological models with observations at different open ocean places, pointing out that differences in the parameterisation of the vertical diffusion could account for differences in the expected new production as deduced from nutrient fluxes. We consider crucial the horizon at which nitrogen flux is computed. From the present model nitracline simulations are found to be around 40–50 m below thermocline. We estimated the nitrate flux beneath the euphotic layer close to nitracline that is below thermocline. Thus, the nitrogen flux was mainly responding to the nitrate gradient rather than the diffusion gradient.

The material exported downward from the euphotic zone in both simulated stations was compensated with the upward nitrate flow (Fig. 13). The averaged daily budget of nitrogen fluxes among the various compartments of the model integrated over the year and averaged daily, was also calculated and shown in Fig. 14. Total nitrogen (nitrate + nitrite + ammonium) taken up by phytoplankton in the CS case was about twice that in the NEA case (4.67 and 2.15 mmol N m^{-2} per day, respectively), thus explaining higher stocks found in the former. About 83% of phytoplankton were ingested by zooplankton in both cases, similar to the estimated by Tusseau et al. (1997) in the simulation of the Ligurian Sea. The role of zooplankton in exporting material was a little higher in NEA than in the CS (77 and 62% of the phytoplankton ingested, respectively). In both sites, the rate of production of both ammonium by zooplankton and nitrite by phytoplankton

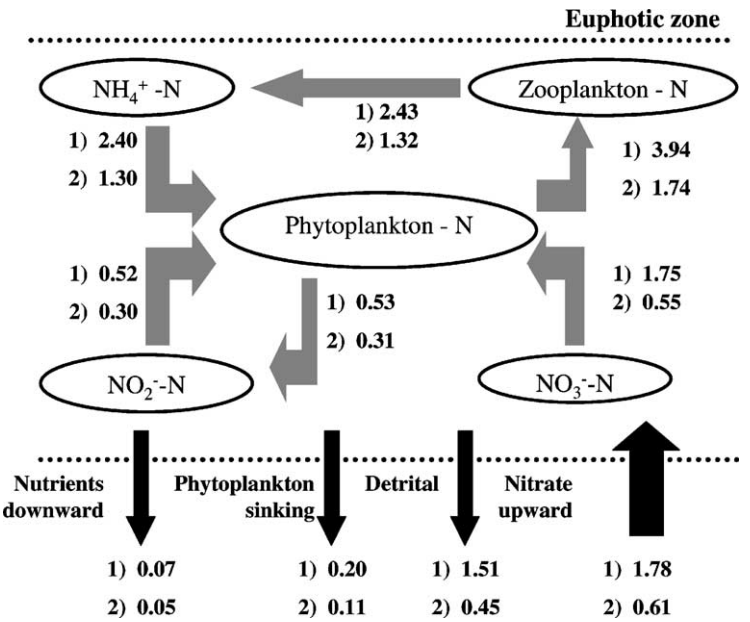

Fig. 13. Mean fluxes of nitrogen (mol N m^{-2} per day) (1) in upper water layers of the Catalan Sea and (2) the subtropical NE Atlantic.

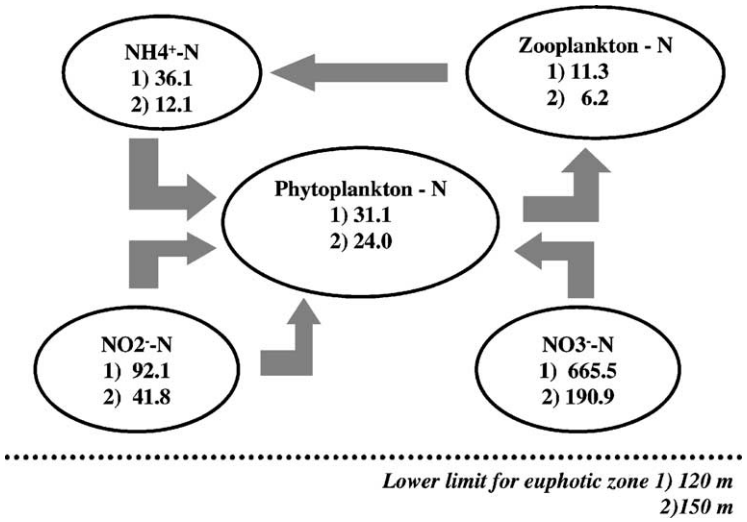

Fig. 14. Annual means of the nitrogen stocks (mmol N m^{-2}) (1) in the euphotic zone of the Catalan Sea and (2) the subtropical NE Atlantic.

were only slightly higher than the rate of uptake by phytoplankton, allowing the observed accumulation in the water column. Nitrogen stocks (Fig. 14) were always higher in the CS than in NEA: zooplankton and nitrite were about twice higher, phytoplankton was about one and half times higher, and ammonium and nitrate were about three times higher in the CS. Most part of nitrate was in the nitrate form with 80% of the nitrogen stock in the CS and 70% in the NEA.

4.4. On the estimates of primary production

The modelled annual primary production in the CS (134.5 g C m^{-2} per year) was in the range of other estimates (94–221 g C m^{-2} per year) using different methods. Based on CZCS imagery, Morel and André (1991) calculated 94 g C m^{-2} per year in the western Mediterranean, similar to the estimates using ^{14}C given by Estrada (1985). A further revision of the CZCS imagery gave higher values of 157.7 g C m^{-2} per year (Antoine et al., 1995). From a photosynthesis–irradiance relationship model, taking into account a large set of chlorophyll and irradiance profiles and satellite images, Sathyendranath et al. (1995) estimated for the whole Mediterranean Sea a primary production of 218 g C m^{-2} per year. Platt et al. (1991) gave an average value of 180 g C m^{-2} per year close to the estimation made by Tusseau et al. (1997) with a numerical model of the pelagic domain for the Ligurian Sea. Longhurst et al. (1995) estimated a primary production of 216 g C m^{-2} per year using satellite information. Lohrenz et al. (1988) gave a value of 0.88 g C m^{-2} per day (equivalent to 221 g C m^{-2} per year) from ^{14}C in May just on density fronts in the western Mediterranean.

The total estimate of primary production by the model in the NEA site was 62.4 g C m^{-2} per year, in the low side of the estimates given by other authors. Platt and Harrison (1985) estimated an annual average primary production of 82 ± 22 g C m^{-2} per year with an average new production (25 ± 7 g C m^{-2} per year) higher than our estimate (16.5 g C m^{-2} per year). The eastern boundary of the subtropical North Atlantic gyre corresponds to a biogeochemical province as described by Sathyendranath et al. (1995) with a mesoscale primary production around 122–124 g C m^{-2} per year (Longhurst et al., 1995) that is twice our estimates. Nevertheless, field measurements of primary production in this area in May and October by Marañón et al. (2000) yielded values in the range of 0.1–0.3 g C m^{-2} per day within the daily average obtained in our simulations (0.14 g C m^{-2} per day). Differences of our model results with other estimates of primary production can be explained in part by the current parameterisation and modelling and by the presence of other external sources of

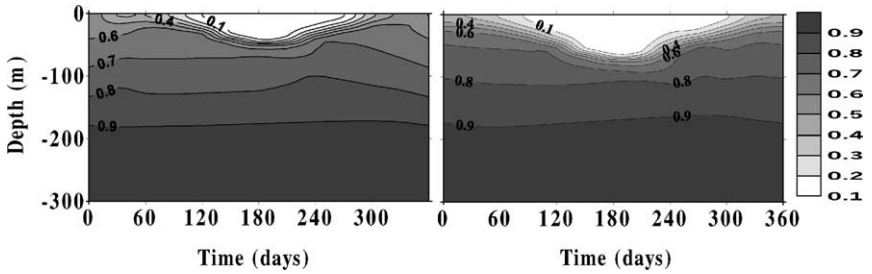

Fig. 15. Depth and time evolution of the *f*-ratio in the Catalan Sea (left) and the subtropical NE Atlantic (right). The *f*-ratio was assumed to be the ratio between the phytoplankton uptake of nitrate (new production) in respect to the whole nitrogen uptake (nitrate+nitrite+ammonium).

nitrogen affecting the primary production, such as the horizontal transport or atmospheric depositions, not included in the present study.

The simulated time evolution of the *f*-ratio along the water column is shown in Fig. 15. Low new production (*f*-ratio = 0.2–0.3) took place just in and above the continuous DCM layer, where nitrate concentrations were very low. The yearly *f*-ratio in the CS was 0.38 with a nitrate-based new production of 51.7 g C m^{-2} per year, similar to an estimate given for the Ligurian Sea (*f*-ratio = 0.35) using a numerical model (Tusseau et al., 1997). In NEA, new production (16.5 g C m^{-2} per year) represents 26% of the total production (*f*-ratio = 0.26). This estimate is twice the estimate given by Williams and Follows (1998) but keep in the range of the expected new production for oligotrophic open oceans. The regenerated production prevailed in summer when nitrate was scarce in the euphotic zone (*f*-ratio = 0.25 and 0.21, in the CS and NEA, respectively) matching the summer estimates given by Bahamón (2002) in the subtropical North Atlantic (*f*-ratio = 0.21). On the contrary, a relatively high new production predominated in autumn and winter times in both locations (0.88–0.82) with the increasing of nitrate in the upper waters by the vertical mixing processes bringing up nitrate from deeper waters.

Since the present model results reasonably match other estimates of primary production and nitrogen fluxes, the model can be assumed to have an adequate parameterisation of the turbulent environment and biogeochemical processes taking place in upper water layers of the selected ecosystems. Using different turbulence schemes to assess primary production in the vertical dimension in the North Sea, Chen and Annan (2000) found that physical differences of the mixing schemes are often smaller than those of biogeochemical features of a modelled ecosystem. This led them to suggest the modelled biogeochemical features as good indicators for a suitable model parameterisation. Gnanadesikan et al. (2002) compared different ecological models with observations at different open ocean places, pointing out that field observations vary more than estimates from different model schemes.

5. Summary and conclusions

The pelagic ecosystem functioning was modelled to have a yearly input of inorganic nitrate from below the euphotic layer compensated with downward losses of material, making the ecosystems in NW Mediterranean and subtropical NE Atlantic to be near the metabolic balance. The simulations of nitrogen stocks and fluxes in both ecosystems were carried out using a similar physical and biogeochemical parameterisation. However, different surface radiation and length of the daylight and different nitrate concentrations in the bottom boundary affected the selected stations located at different latitudes. Higher irradiance and daylight length making the euphotic layer thicker explained that the phytoplankton maximum was deeper in NEA than in CS during summertime. In both locations zooplankton grazing controlled the late winter phytoplankton bloom but reduced more than expected the subsurface phytoplankton concentration in summer. In general, the variables better assessed in the model were chlorophyll *a*, nitrate and nitrite, close to time and depth observations. The amount of irradiance appears to control the chlorophyll maximum depth

while the amount of nitrate at the bottom boundary is mainly controlling the phytoplankton stocks. DCM was found more linked to nutricline depth variation than to thermocline depth. Close to DCM was found the nitrite maximum whose concentrations were explained by the phytoplankton exudation in the dark. The upward fluxes of nitrate below the euphotic zone in the CS and NEA stations were in agreement with previous estimates suggesting a suitable parameterisation of the density field and turbulent diffusion. The estimates of nitrate fluxes were more attributable to the nitrate gradient than to the density field.

Acknowledgements

This work was partly funded by the European Commission through project MFSPP: *Mediterranean Forecasting System, Pilot Project* (MAS3-CT98-0171). The Spanish Agency for International Co-operation provided partial financial support for N.B. Z.R. Velásquez kindly supplied all chlorophyll concentration data in the database. Special thanks are due to L.J. Simic who organised the database, and who accidentally died while this paper was being prepared. Comments by two anonymous reviewers and the editor greatly improved the present manuscript.

References

Alcaraz, M., 1988. Summer zooplankton metabolism and its relation to primary production in the Western Mediterranean. Oceanol. Acta SP 185–191.

Antoine, D., Moreland, A., André, J.-M., 1995. Algal pigment distribution and primary production in the Eastern Mediterranean as derived from coastal zone color scanner observations. J. Geophys. Res. 100, 16193–16209.

Aufdenkampe, A.K., McCarthy, J.J., Navarette, C., Rodier, M., Dunne, J., Murray, J.W., 2002. Biogeochemical controls on new production in the tropical Pacific. Deep-Sea Res. II 49, 2619–2648.

Bahamón, N., 2002. Dynamics of oligotrophic pelagic ecosystems: NW Mediterranean and subtropical NE Atlantic. Ph.D. Dissertation, Universitat Politècnica de Catalunya, Barcelona, 172 pp.

Baker, K.S., Frouin, R., 1987. Relation between photosynthetically available radiation and total insulation at the ocean surface under clear skies. Limnol. Oceanogr. 32, 1370–1377.

Berges, J.A., Falkowski, P.G., 1998. Physiological stress and cell death in marine phytoplankton: induction of proteases in response to nitrogen or light limitation. Limnol. Oceanogr. 43, 129–135.

Blasco, D., 1971. Composición y distribución del fitoplancton en la región del afloramiento de las costas peruanas. Inv. Pesq. 35, 61–112.

Bricaud, A., Morel, A., Tailliez, D., 1992. Mesures optiques. In: Neveux, J. (Ed.), Les Maximums Profonds de chl a en mer des Sargasses. Données physiques, chimiques et biologiques. Campagne Chlomax, Campagnes Océanographiques Françaises No. 17. CNRS-Groupe de Recherche P4, Banyuls-sur-Mer, France, pp. 39–47.

Brock, T.D., 1981. Calculating solar radiation for ecological studies. Ecol. Model. 14, 1–19.

Carlucci, A.F., Hartwig, E.O., Bowes, P.M., 1970. Biological production of nitrite in seawater. Mar. Biol. 7, 161–166.

Carril, A.F., Menéndez, C.G., Nuñez, M.N., 1997. Climate change scenarios over the South American Region: an intercomparison of coupled general atmosphere–ocean circulation models. Int. J. Climatol. 17, 1613–1633.

Chen, F., Annan, J.D., 2000. The influence of different turbulent schemes on modelling primary production in a 1D coupled physical–biological model. J. Mar. Syst. 26, 259–288.

Cruzado, A., 1982. Simulation model of primary production in coastal upwelling off Western Sahara. Rapp. P.-V. Réun. Cons. Int. Explor. Mer 180, 228–233.

Cruzado, A., Kelley, J.C., 1974. Continuous measurements of nutrient concentrations and phytoplankton density in the surface water of the western Mediterranean Sea, winter 1970. Thalassia Jugoslavica 9 (1/2), 19–24.

Denman, K.L., Platt, T., 1977. Biological prediction in the sea. In: Kraus, E.B. (Ed.), Modelling and Prediction of the Upper Layers of the Ocean. Pergamon Press, Oxford, pp. 251–262.

Denman, K.L., Gargett, A.E., 1983. Time and space scales of vertical mixing and advection of phytoplankton in the upper ocean. Limnol. Oceanogr. 28, 801–815.

Doney, S.C., 1999. Major challenges confronting marine biogeochemical modeling. Global Biogeochem. Cycles 13 (3), 705–714.

Doney, S.C., Glover, D.M., Najjar, R.G., 1996. A new coupled, one-dimensional biological–physical model for the upper ocean: applications to the JGOFS Bermuda Atlantic Time-Series Study (BATS) site. Deep-Sea Res. II 43, 591–624.

Dugdale, R.C., 1967. Nutrient limitation in the sea: dynamics, identification and significance. Limnol. Oceanogr. 12, 685–695.

Dugdale, R.C., Goering, J.J., 1967. Uptake of new and regenerated forms of nitrogen in primary productivity. Limnol. Oceanogr. 12 (2), 6–206.

Edwards, A.M., Yool, A., 2000. Role of higher predation in plankton population models. J. Plankton Res. 22 (6), 1085–1112.

Eppley, R.W., Peterson, B.J., 1979. Particulate organic matter flux and planktonic new production in the deep ocean. Nature 282, 677–680.

Estrada, M., 1985. Primary production at the deep chlorophyll maximum in the western Mediterranean. In: Gibbs, P.E. (Ed.), Proceeding of the 19th European Marine Biology Symposium. Cambridge University Press, Cambridge, pp. 109–121.

Estrada, M., Varela, R.A., Salat, J., Cruzado, A., Arias, E., 1999. Spatio-temporal variability of the winter phytoplankton distribution across the Catalan and North Balearic fronts (NW Mediterranean). J. Plankton Res. 21 (1), 1–20.

Evans, G.T., 1999. The role of local models and data sets in the Joint Global Ocean Flux Study. Deep-Sea Res. I 46, 1369–1389.

Evans, G.T., Parslow, J.S., 1985. A model of annual plankton cycles. Biol. Oceanogr. 3, 327–347.

Fasham, M.R., Ducklow, H.W., McKelvie, S.M., 1990. A nitrogen-based model of plankton dynamics in the oceanic mixed layer. J. Mar. Res. 48 (3), 591–639.

Gnanadesikan, A., Slater, R.D., Gruber, N., Sarmiento, J.L., 2002. Oceanic vertical exchange and new production: a comparison between models and observations. Deep-Sea Res. II 49, 363–401.

Goericke, R., Welschmeyer, N.A., 1998. Response of Sargasso Sea phytoplankton, phytoplankton, growth rates and primary production to seasonally varying physical forcing. J. Plankton Res. 20 (12), 2223–2249.

Gruber, N., Sarmiento, J.L., 1997. Global patterns of marine nitrogen fixation and denitrification. Global Biogeochem. Cycles 11, 235–266.

Herbland, A., Voituriez, B., 1979. Hydrological structure analysis for estimating the primary production in the tropical Atlantic Ocean. J. Mar. Res. 37, 87–102.

Hurtt, G.H., Armstrong, R.A., 1996. A pelagic ecosystem model calibrated with BATS data. Deep-Sea Res. II 43 (2/3), 653–683.

Jenkins, W., 1988. Nitrate flux into the euphotic zone near Bermuda. Nature 331, 521–523.

Kiefer, D.A., Kremer, J.N., 1981. Origins of vertical patterns of phytoplankton and nutrients in the temperate open ocean: a stratigraphic hypothesis. Deep-Sea Res. 28, 1087–1105.

Levy, M., Memery, L., Andre, J.-H., 1998. Simulation of primary production and export fluxes in the northwestern Mediterranean Sea. J. Mar. Res. 56 (1), 197–238.

Lewis, M.R., Harrison, W.G., Oakey, N.S., Hebert, D., Platt, T., 1986. Vertical nitrate fluxes in the oligotrophic ocean. Science 234, 870–873.

Lohrenz, S.E., Wiesenburg, D.A., DePalma, I.P., Johnson, K.S., Gustafson, D.E., 1988. Interrelationships among primary production, chlorophyll, and environmental conditions in frontal regions of the western Mediterranean Sea. Deep-Sea Res. 35 (5), 793–810.

Longhurst, A., Sathyendranath, S., Platt, T., Caverhill, C., 1995. An estimate of global primary production in the ocean from satellite radiometer data. J. Plankton Res. 17 (6), 1245–1271.

Marañón, E., Holligan, P.M., Varela, M., Mouriño, B., Bale, A.J., 2000. Basin-scale variability of phytoplankton biomass production and growth in the Atlantic Ocean. Deep-Sea Res. I 47, 825–857.

Marra, J., Bidigare, R.R., Dickey, T.D., 1990. Nutrients and mixing, chlorophyll and phytoplankton growth. Deep-Sea Res 37 (1), 127–143.

McGillicuddy, D.J., Robinson, A.R., 1997. Eddy-induced nutrient supply and new production in the Sargasso Sea. Deep-Sea Res. I 8, 1427–1450.

Menzel, D.W., Ryther, J.H., 1960. The annual cycle of primary production in the Sargasso Sea off Bermuda. Deep-Sea Res. 6, 351–367.

Menzel, D.W., Ryther, J.H., 1961. Annual variation in primary production of the Sargasso Sea off Bermuda. Deep-Sea Res. 7, 282–288.

Millero, F.J., Poisson, A., 1981. International one-atmosphere equation of state of sea water. Deep-Sea Res. 28A (6), 625–629.

Morel, A., André, J.-M., 1991. Pigment distribution and primary production in the western Mediterranean, as derived and modeled from coastal zone color scanner observations. J. Geophys. Res. 96, 12685–12698.

Morel, A., Ahn, Y.-W., Partensky, F., Vaulot, D., Claustre, H., 1993. *Prochlorococcus* and *Synechococcus*: a comparative study of their size, pigmentation and related optical properties. J. Mar. Res. 51, 617–649.

Oguz, T., Ducklow, H., Malanotte-Rizzoli, P., Tugrul, S., Nezlin, N.P., Unluata, U., 1996. Simulation of annual plankton productivity cycle in the Black Sea by a one-dimensional physical–biological model. J. Geophys. Res. 101 (C7), 16585–16599.

Oguz, T., Malanotte-Rizzoli, P., Ducklow, H.W., 2001. Simulations of phytoplankton seasonal cycle with multi-level and multi-layer physical–ecosystem models: the Black Sea example. Ecol. Model. 144, 295–314.

Osborn, T.R., 1980. Estimates of the local rate of vertical diffusion from dissipation measurements. J. Phys. Oceanogr. 10 (1), 83–89.

Owen, R.W., 1981. Fronts and eddies in the sea: mechanisms, interactions and biological effects. In: Longhurst, A.R. (Ed.), Analysis of Marine Ecosystems. Academic Press, London, pp. 197–233.

Pedrós-Alió, C., Calderón-Paz, J.-I., Guixa-Boixereu, N., Estrada, M., Gasol, J.M., 1999. Bacterioplankton and phytoplankton biomass and production during summer stratification in the northwestern Mediterranean Sea. Deep-Sea Res. I 46, 985–1019.

Planas, D., Agustí, S., Duarte, C., Granata, T., 1999. Nitrate uptake and diffusive nitrate supply in the Central Atlantic. Limnol. Oceanogr. 44 (1), 116–126.

Platt, T., Harrison, W.G., 1985. Biogenic fluxes of carbon and oxygen in the ocean. Nature 318, 55–58.

Platt, T., Caverhill, C., Sathyendranath, S., 1991. Basin-scale estimates of oceanic primary production by remote sensing: the North Atlantic. J. Geophys. Res. 96, 15147–15159.

Raimbault, P., 1986. Effect of temperature on nitrite excretion by three marine diatoms during nitrate uptake. Mar. Biol. 92, 149–155.

Rastetter, E.B., 1996. Validating models of ecosystem response to global change. How can we best assess models of long-term global change? Bioscience 46 (3), 190–198.

Salat, J., 1995. The interaction between the Catalan and Balearic currents in the southern Catalan Sea. Oceanol. Acta 18 (2), 227–234.

Sarmiento, J.L., Slater, R.D., Fasham, M.R.J., Ducklow, H.W., Toggweiler, J.R., Evans, G.T., 1993. A seasonal three-dimensional ecosystem model of nitrogen cycling in the North Atlantic euphotic zone. Global Biogeochem. Cycles 7, 417–450.

Sathyendranath, S., Longhurst, A., Caverhill, C.M., Platt, T., 1995. Regionally and seasonally differentiated primary production in the North Atlantic. Deep-Sea Res. I 42 (10), 1773–1802.

Sharples, J., 1999. Investigating the seasonal vertical structure of phytoplankton in shelf seas. Marine Models 1, 3–38.

Sharples, J., Moore, C.M., Rippeth, T.P., Holligan, P.M., Hydes, D.J., Fisher, N.R., Simpson, J.H., 2001. Phytoplankton distribution and survival in the thermocline. Limnol. Oceanogr. 46 (3), 486–496.

Skogen, M.D., Svendsen, E., Berntsen, J., Aksnes, D., Ulvestad, K.B., 1995. Modelling the primary production in the North Sea using a coupled three-dimensional physical–chemical–biological ocean model. Estuarine, Coastal Shelf Sci. 41, 545–565.

Steele, J., 1977. Ecological modelling of the upper layers. In: Kraus, E.B. (Ed.), Modelling and Prediction of the Upper Layers of the Ocean. Pergamon Press, Oxford, pp. 243–250.

Tusseau, M.H., Lancelot, C., Martin, J.M., Tassin, B., 1997. 1-D coupled physical–biological model of the northwestern Mediterranean Sea. Deep-Sea Res. II 44 (3/4), 851–880.

Vaccaro, R.F., Ryther, J.H., 1960. Marine phytoplankton and the distribution of nitrite in the sea. J. Cons. Perm. Int. Explor. Mer 25, 260–271.

Varela, R., Cruzado, A., Tintoré, J., García, E., 1992. Modelling the deep-chlorophyll maximum: a coupled physical–biological approach. J. Mar. Res. 50, 441–463.

Varela, R.A., Cruzado, A., Tintore, J., 1994. A simulation analysis of various biological and physical factors influencing the deep-chlorophyll maximum structure in oligotrophic areas. J. Mar. Syst. 5, 1–15.

Velásquez, Z.R., 1997. Fitoplancton en el Mediterráneo noroccidental. Ph.D. Dissertation, Universidad Politécnica de Cataluña, Barcelona, 271 pp.

Williams, R.G., Follows, M.J., 1998. The Ekman transfer of nutrients and maintenance of new production over the North Atlantic. Deep-Sea Res. I 45, 461–489.

Zakardjian, B., Prieur, L., 1994. A numerical study of primary production related to vertical turbulent diffusion with special reference to vertical motions of the phytoplankton cells in nutrients and light fields. J. Mar. Syst. 5, 267–295.

Zakardjian, B., Prieur, L., 1998. Biological and chemical signs of upward motions in permanent geostrophic fronts of the Western Mediterranean. J. Geophys. Res. 103 (C12), 27849–27866.